

## Limits on Fluorescence Detected Circular Dichroism of Single Helicene Molecules

Yiqiao Tang,<sup>†</sup> Timothy A. Cook,<sup>‡,§</sup> and Adam E. Cohen<sup>\*,†,‡</sup>*Department of Physics, Harvard University, Cambridge, Massachusetts 02138, and Department of Chemistry and Chemical Biology, Harvard University, Cambridge, Massachusetts 02138**Received: April 19, 2009; Revised Manuscript Received: May 6, 2009*

Fluorescent imaging of single helicene molecules is applied to study the optical activity of chiral fluorophores. In contrast to the previous report by Hassey et al. (*Science* **2006**, *314*, 1437), the dissymmetry factors of single chiral fluorophores are found not to differ significantly from the bulk value of  $|g| < 10^{-4}$  at 457 nm. Linear dichroism and birefringence of the dichroic mirror inside the fluorescence microscope change the polarization state of the incoming laser beam significantly; i.e., circular polarized light sent into the microscope becomes highly elliptically polarized after reflection from the dichroic mirror. Compensation for this effect should be made to avoid artifacts brought by linear dichroism in single immobilized molecules.

Single-molecule measurements have been used to probe the states and dynamics of a huge variety of biophysical and condensed matter systems,<sup>2–4</sup> and often yield information that is missed by bulk, ensemble-averaged techniques. In particular, measurements at ambient and low temperatures provide detailed information about the interactions between single fluorescent molecules and their local environment. The heterogeneously broadened lines visible in bulk often resolve into much narrower single-molecule lines, which show spectral diffusion,<sup>5,6</sup> blinking,<sup>7</sup> and polarization fluctuations<sup>8,9</sup> that indicate complex interactions with the host.

Chiral molecules of a single enantiomer show differential absorption of left and right circularly polarized light (CPL). The degree of circular dichroism (CD) at a particular frequency is measured by the  $g$ -value:

$$g \equiv \frac{2(\Gamma^+ - \Gamma^-)}{(\Gamma^+ + \Gamma^-)}$$

where  $\Gamma^\pm$  is the rate of excitation in right (+) or left (-) CPL. The  $g$ -value varies between  $-2 \leq g \leq 2$ . For most small organic molecules, peptides, nucleic acids, and sugars,  $|g| < 10^{-3}$  in the visible.<sup>10</sup> The smallness of  $g$  arises from the small size of molecules relative to the helical pitch of CPL: the electromagnetic field undergoes a nearly imperceptible twist over a distance of molecular dimensions.

At the quantum mechanical level, CD arises through an interference between electric dipole and either electric quadrupole or magnetic dipole transitions.<sup>11</sup> The Hamiltonian relevant to CD for a chiral molecule in an electromagnetic field is:<sup>12–14</sup>

$$H = -\boldsymbol{\mu} \cdot \mathbf{E} - \boldsymbol{\theta} : \nabla \mathbf{E} - \mathbf{m} \cdot \mathbf{B}$$

where  $\boldsymbol{\mu}$  is the electric dipole operator,  $\boldsymbol{\theta}$  is the electric quadrupole operator, and  $\mathbf{m}$  is the magnetic dipole operator;  $\mathbf{E}$  is the electric field, and  $\mathbf{B}$  is the magnetic field. The rate of excitation from an initial state  $i$  to a final state  $f$  involves the expression  $|\langle f | H | i \rangle|^2$ , as specified by Fermi's golden rule. This expression contains a term proportional to  $|\mu_{if}|^2$ , as well as cross-terms containing  $\boldsymbol{\mu}$  and  $\boldsymbol{\theta}$  or  $\boldsymbol{\mu}$  and  $\mathbf{m}$  (the remaining terms are small enough to be neglected). The term containing  $|\mu_{if}|^2$  represents electric dipole absorption, and is not sensitive to molecular chirality. The signs of the two cross-terms, however, depend on molecular chirality, so these terms are responsible for circular dichroism. Both cross-terms depend on the orientation of the molecule relative to the incident field. Upon averaging over all molecular orientations, the electric quadrupole contribution to the differential absorption averages to zero while the magnetic dipole term remains.<sup>13</sup> Thus, electric quadrupole transitions do not contribute to bulk CD, while magnetic dipole transitions do contribute.

In light of the increased information available from single-molecule measurements, it is interesting to compare the chiroptical response of a single chiral molecule to the ensemble-averaged response. One can measure chiroptical effects in small samples by using fluorescent chiral molecules.<sup>15,16</sup> The rate of fluorescence emission is proportional to the rate of excitation, and thus, fluorescence detected circular dichroism (FDCD) provides a possible probe of chiroptical effects at the single-molecule level. Single-molecule FDCD might differ from bulk FDCD for several reasons:

(1) Electric quadrupole and magnetic dipole matrix elements of orientationally fixed single molecules may differ from their rotationally averaged values in bulk systems.<sup>13,17</sup>

(2) Local interactions with the host could modify the oscillator strengths or frequencies of the electric quadrupole or magnetic dipole transitions, to induce molecule-to-molecule variations in CD, i.e., heterogeneous broadening of CD lines.

The smallness of the electric quadrupole and magnetic dipole contributions to the Hamiltonian is purely geometrical in origin,

\* To whom correspondence should be addressed. E-mail: cohen@chemistry.harvard.edu.

<sup>†</sup> Department of Physics.

<sup>‡</sup> Department of Chemistry and Chemical Biology.

<sup>§</sup> Current address: School of Law, University of Virginia, Charlottesville, VA 22903.

a consequence of the small size of a molecule relative to the wavelength of light. Orientational averaging reduces the strength of the electric dipole/magnetic dipole interference by a factor of 3 relative to its peak value.<sup>13</sup> Electric quadrupole transitions average to zero in bulk, so bulk measurements provide no guidance on their magnitude. Geometrical considerations, however, indicate that the electric quadrupole term should be of the same order of magnitude as the magnetic dipole term. Density functional simulations of single helicene molecules support the prediction that single-molecule  $g$ -values are of the order of  $10^{-3}$ , of the same order as in bulk at the same excitation wavelength.<sup>18</sup>

Nonetheless, theoretical models may be wrong, so there was considerable interest in the report from Hassey et al.<sup>1</sup> that single molecules of bridged triarylamine helicenes show  $g$ -values ranging from +2 to -2, while in bulk the two enantiomers have  $|g| < 10^{-4}$  at a probe wavelength of 457 nm. Furthermore, they reported that both enantiomers of this compound show very similar broad distributions of single-molecule  $g$ -values, and that the wavelength dependence of the single-molecule  $g$ -values does not correspond to the bulk, even when averaged over many single molecules.<sup>18</sup>

We attempted to replicate the experiments of Hassey et al. and initially saw similar broad distributions of  $g$ -values. However, after correcting for the linear birefringence and linear dichroism inherent to the dichroic mirrors used in single-molecule FDCD experiments, the distribution of  $g$ -values collapses to a sharp distribution around  $g = 0$ . The uncertainty in the measurements does not allow us to distinguish the  $g$ -values of opposite enantiomers.

## Methods

Triarylamine helicenes M-2 and P-2 (Figure 1a) were synthesized following literature procedures<sup>19,20</sup> with modifications. (2-Methoxyphenyl)-naphthalenylamine was synthesized using (1,1'-bis(diphenylphosphino)ferrocene)PdCl<sub>2</sub>·CH<sub>2</sub>Cl<sub>2</sub> as the amination catalyst,<sup>21</sup> and deprotection of the helicene methyl ether was accomplished using BBr<sub>3</sub>.<sup>22</sup> The molecules we prepared are identical to the ones Hassey et al. used in ref 1.

The products were characterized by <sup>1</sup>H NMR, <sup>13</sup>C NMR, and mass spectrometry; all data match the literature spectra. The circular dichroism (Figure 1b) and fluorescence (not shown) spectra are identical to earlier reports.<sup>19</sup> Both enantiomers show strong FDCD in bulk when excited with light at 355 nm, with  $g$ -values of  $+8.0 \times 10^{-3}$  for M-2 and  $-8.1 \times 10^{-3}$  for P-2. At 457 nm, the wavelength used in the experiments of Hassey et al., the  $g$ -values are  $|g| < 10^{-4}$ .

Following the procedure of Hassey et al., we made solutions of the helicenes at  $10^{-8}$  M in methanol and drop-cast these solutions onto a Zeonor film (ZF-14 ZEONEX/ZEONOR). A fused silica coverslip was cleaned in Piranha solution (3:1 H<sub>2</sub>SO<sub>4</sub>: H<sub>2</sub>O<sub>2</sub>, *Caution*: highly corrosive). The Zeonor film was placed, helicene side down, onto the coverslip, and the samples were imaged in an inverted single-molecule fluorescence microscope.

The optical setup is shown in Figure 2a. The setup is built around an Olympus IX71 inverted fluorescence microscope. The light source is a Melles Griot argon-ion laser operating at 457 nm (0.4 mW at the sample). A narrow-band excitation filter (D457/10x Chroma) is used to remove plasma emission at other wavelengths. The light is polarized by a Glan Thompson polarizer (10GL08 Newport), passed through a liquid crystal variable retarder (LCVR, LRC - 200 - VIS, Meadowlark Optics), and then through a quarter wave Fresnel rhomb retarder

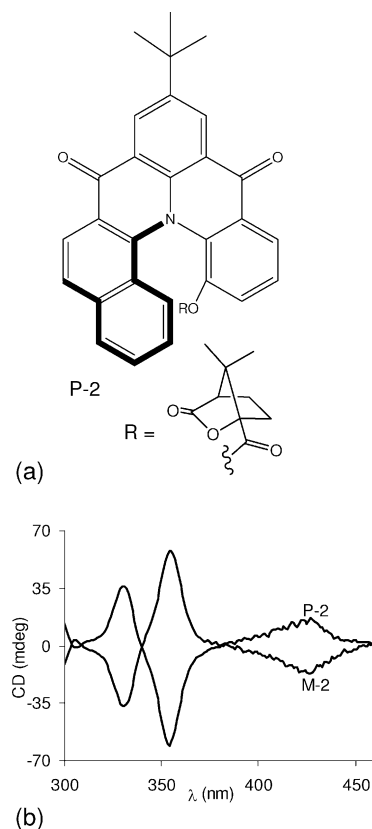


**Figure 1.** Bridged triarylamine helicenes. (a) Structure of the P-2 enantiomer. The camphanate group is used as a chiral resolving agent and renders the M-2 and P-2 species technically diastereomers. However, the camphanate group has no detectable effect on the optical properties of either species. (b) Circular dichroism spectrum of M-2 and P-2, measured with a JASCO CD spectrometer. The spectrum of the P-2 was scaled by a constant factor to correct for a slight difference in concentration between the two samples.

(FM600QM Thorlabs). The LCVR is driven with a 2 kHz square wave. An arbitrary state of ellipticity is generated by adjusting the LCVR drive voltage. We have mirrors between the polarizer and the microscope, to avoid introducing spurious phase shifts onto the beam. The only reflection after the initial polarizer is off the dichroic mirror.

A lens with a focal length of 15 cm (LA1433-A Thorlabs) brings the light to a focus at the back focal plane of the objective. After passing through the lens, the light is deflected upward by a dichroic mirror. We performed experiments using either of two dichroics: DC1, 460 nm long pass; DC2 (Olympus DM500), 500 nm long pass. Our objective lens is a 60 $\times$ , N.A. 1.45, oil immersion, plan apochromat (1-U2B616 Olympus). Fluorescence from the sample is collected by the same objective, passed through the dichroic mirror, and separated from the excitation light by a 470 nm long-pass emission filter (HQ470LP Chroma). Images are collected on an Andor iXon<sup>+</sup> electron-multiplying CCD (DU-897E-CS0-#BV), cooled to  $-50$  °C.

A program written in LabView synchronizes the acquisition of images with the application of voltages to the LCVR. The LCVR has an  $\sim 30$  ms response time to a change in the amplitude of its driving voltage, so each image acquisition starts 100 ms after a change in the voltage on the LCVR. In a typical experiment, 40 images are acquired, at 400 ms exposure per frame, with a switch in the polarization state between each frame. An amplified photodiode detector (PDA36A, Thorlabs) is mounted on top of the microscope to monitor the intensity

of the transmitted laser beam. This photodetector allows us to correct for laser power fluctuations.

Prior to each experiment, we measure the polarization state of the light entering the microscope and emerging from the objective. A polarizer (GL10 Thorlabs) is temporarily placed in the beam path at the point of measurement. The transmitted intensity is recorded using a power meter (FieldMaxII-TO Coherent Inc.) as a function of the angle of the polarizer.

Data are acquired under two conditions for each enantiomer: alternating left- and right-CPL sent into the microscope and alternating left- and right-CPL at the sample plane. The analysis for all movies is completely automated using custom software written in Matlab, with identical parameters for all data sets. Thus, there is no possibility for bias in selecting molecules or extracting their intensities.

## Results

Figure 2b shows an image of single helicene molecules on the Zeonor film. We first imaged the molecules with alternating left- and right-CPL sent into the microscope. For both polarizations, the ellipticity before the microscope is greater than 96%. Many molecules show strong asymmetries in their brightness, as shown in Figure 3b, leading to apparent  $g$ -values ranging from  $-2$  to  $2$ . However, under these conditions the light emerging from the microscope is not circularly polarized. Ellipticities are 36% for DC1 and 55% for DC2.

To generate CPL *at the sample*, we measured the Jones matrices<sup>23</sup> for the dichroics. They are

$$\begin{pmatrix} 1 & 0 \\ 0 & 1.34e^{0.79i} \end{pmatrix}$$

and

$$\begin{pmatrix} 1 & 0 \\ 0 & 0.97e^{0.39i} \end{pmatrix}$$

for DC1 and DC2, respectively. We solved the matrix equations to identify the Jones vectors of the input polarization states which lead to CPL at the sample. These are

$$\frac{1}{1.25} \begin{pmatrix} 1 \\ \pm 0.75e^{0.78i} \end{pmatrix}$$

for DC1 and

$$\frac{1}{1.43} \begin{pmatrix} 1 \\ \pm 1.03e^{1.18i} \end{pmatrix}$$

for DC2. These polarizations are generated by applying appropriate voltages to the LCVR. Measurements confirmed ellipticities  $>96\%$  above the sample for both right- and left-CPL.

Figure 3b shows a histogram of  $g$ -values measured for single molecules with CPL before the microscope (using DC1) and with CPL at the sample (using DC2). The apparent  $g$ -values are broadly distributed in the case where the CPL is generated before the microscope, using either DC2 (data not shown) or DC1. In contrast, with CPL at the sample, the  $g$ -values are not significantly different from zero:  $g = 0.026 \pm 0.27$  for M-2 and  $g = 0.033 \pm 0.29$  for P-2. The width of the observed distribution is largely due to statistical uncertainties in the extraction of single-molecule  $g$ -values in the presence of shot-noise and molecular blinking and photobleaching. Thus, current experimental techniques cannot detect deviations from 0 in the  $g$ -values of single helicene molecules measured at 457 nm.

## Discussion

We have shown that the broad distribution of  $g$ -values observed by Hassey et al. can be explained by *linear dichroism*<sup>24</sup> in the randomly oriented helicene molecules, coupled with imperfect circular polarization of the illumination. We believe that such a mechanism is a more probable explanation for their data than is anomalously large circular dichroism at the single-molecule level, which would require a hitherto unknown physical effect. In addition to the dichroic mirrors discussed above, a third dichroic mirror with a cutoff of 570 nm (Olympus DM570) also shows strong linear birefringence for 532 nm light. We conclude that strong linear birefringence is a general feature of dichroic mirrors. Finding a dichroic with nearly equal

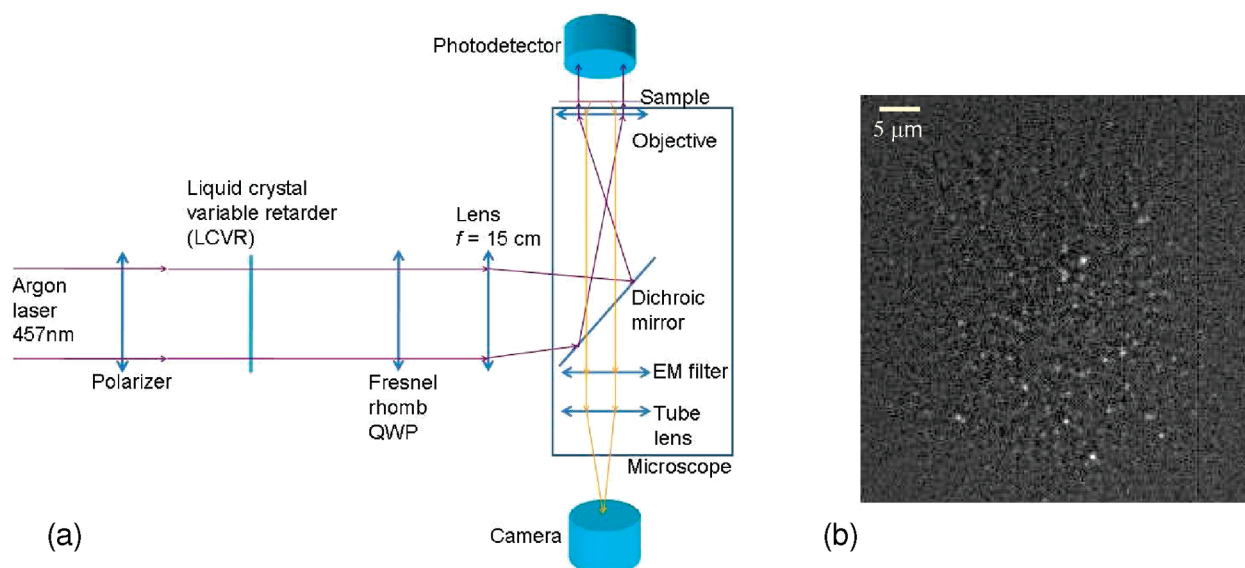


**Figure 2.** Imaging of single helicene molecules under light of controlled polarization. (a) Schematic diagram of optical setup for wide-field imaging. See text for a detailed description. (b) Image of single helicene molecules. A diffuse background image, calculated using a 2-dimensional median filter, was subtracted from the raw image to enhance the contrast of the single molecules.

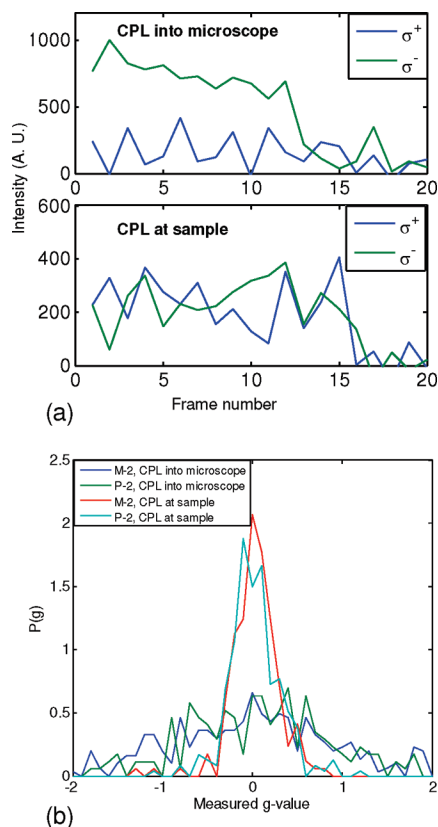


**Figure 3.** Fluorescence of single helicene molecules in CPL. (a) Time-traces of single helicene molecules with CPL sent into the microscope (top) and CPL generated at the sample plane (bottom). There is a large apparent  $g$ -value when CPL is sent into the microscope but not when CPL is generated at the sample. Both molecules show single-step photobleaching. (b) Histogram of  $g$ -values for both enantiomers, under both polarization conditions. With CPL at the sample, the  $g$ -values are much more narrowly distributed. The number of molecules measured for each histogram are the following: M-2 CPL in, 303; P-2 CPL in, 173; M-2 CPL out, 169; P-2 CPL out, 234.

reflectivities for  $s$ - and  $p$ -polarized light (such as our dichroic DC2) is not sufficient to preserve the polarization state of incident light; the phase shift between  $s$ - and  $p$ -polarizations is important too. An observation of CPL in light back-reflected from the sample is also not proof of CPL at the sample, because the back-reflected light has undergone a second phase-shifting reflection at the dichroic.

If CPL is sent into a fluorescence microscope, the dichroic mirror converts this light into elliptically polarized light at the sample, with different principal axes arising from the two input circular polarizations. The linearly polarized component of this illumination leads to different rates of pure electric dipole excitation for each randomly oriented molecule. Many authors have documented the perils of performing microscopic CD measurements.<sup>14,23,25</sup> Claborn and co-workers avoided any

reflective elements in their optical train and so were not subject to this source of error.<sup>25</sup>

Circular dichroism measurements at the single-molecule level promise important information on molecular structure and local environmental interactions. However, uncompensated linear birefringence and linear dichroism in optical elements inside a microscope can cause linear dichroism to masquerade as circular dichroism. Caution is advised in performing and interpreting such experiments.

**Acknowledgment.** We thank Prashant Jain and Sijia Lu for helpful discussions, Charles Lieber and Sunney Xie for loans of equipment, and Gregory Verdine for use of the CD spectrometer. We thank Michael Barnes for comments on an early draft of this manuscript. This work was partially supported by a Dreyfus New Faculty Award and the MITRE Corporation and the U.S. Government's Nano-Enabled Technology Initiative.

## References and Notes

- (1) Hassey, R.; Swain, E. J.; Hammer, N. I.; Venkataraman, D.; Barnes, M. D. *Science* **2006**, *314*, 1437.
- (2) Moerner, W. E.; Kador, L. *Phys. Rev. Lett.* **1989**, *62*, 2535.
- (3) Moerner, W. E. *Proc. Natl. Acad. Sci. U.S.A.* **2007**, *104*, 12596.
- (4) Selvin, P. R.; Ha, T. *Single Molecule Techniques: A Laboratory Manual*; Cold Spring Harbor Laboratory Press: New York, 2007.
- (5) Bauer, M.; Kador, L. *J. Chem. Phys.* **2004**, *120*, 10278.
- (6) Vainer, Y. G.; Naumov, A. V. *Opt. Spectrosc.* **2005**, *98*, 747.
- (7) Dickson, R. M.; Cubitt, A. B.; Tsien, R. Y.; Moerner, W. E. *Nature* **1997**, *388*, 355.
- (8) Le Floch, V.; Brasselet, S.; Roch, J. F.; Zyss, J. *J. Phys. Chem. B* **2003**, *107*, 12403.
- (9) Dickson, R. M.; Norris, D. J.; Moerner, W. E. *Phys. Rev. Lett.* **1998**, *81*, 5322.
- (10) Inoue, Y.; Ramamurthy, V. *Chiral Photochemistry (Molecular and Supramolecular Photochemistry)*; CRC Press: New York, 2004.
- (11) Schellman, J. A. *Chem. Rev.* **1975**, *75*, 323.
- (12) Barron, L. D. *Molecular Light Scattering and Optical Activity*; Cambridge University Press: Cambridge, U.K., 2004.
- (13) Craig, D. P.; Thirunamachandran, T. *Molecular Quantum Electrodynamics*; Dover Publications: New York, 1998.
- (14) Disch, R. L.; Sverdlik, D. I. *Anal. Chem.* **1969**, *41*, 82.
- (15) Tinoco Jr, I.; Turner, D. H. *J. Am. Chem. Soc.* **1976**, *98*, 6453.
- (16) Turner, D. H.; Tinoco Jr, I.; Maestre, M. *J. Am. Chem. Soc.* **1974**, *96*, 4340.
- (17) Tinoco Jr, I.; Ehrenberg, B.; Steinberg, I. Z. *J. Chem. Phys.* **1977**, *66*, 916.
- (18) Hassey, R.; McCarthy, K. D.; Swain, E.; Basak, D.; Venkataraman, D.; Barnes, M. D. *Chirality* **2008**, *20*, 1039.
- (19) Field, J. E.; Muller, G.; Riehl, J. P.; Venkataraman, D. *J. Am. Chem. Soc.* **2003**, *125*, 11808.
- (20) Field, J. E.; Hill, T. J.; Venkataraman, D.; He, H.; Janso, J. E.; Williamson, R. T.; Yang, H. Y.; Carter, G. T.; Carra, C.; Ghigo, G. *J. Org. Chem.* **2003**, *68*, 6071.
- (21) Driver, M. S.; Hartwig, J. F. *J. Am. Chem. Soc.* **1996**, *118*, 7217.
- (22) Ten equivalents of  $\text{BBr}_3$  (1.0 M in  $\text{CH}_2\text{Cl}_2$ ) were added to a solution of the helicene methyl ether in  $\text{CH}_2\text{Cl}_2$  at 0 °C. The reaction was stirred at 25 °C for 18 h, quenched with saturated aqueous  $\text{NaHCO}_3$ , and worked up as in ref 20. Yield was quantitative.
- (23) Schellman, J.; Jensen, H. P. *Chem. Rev.* **1987**, *87*, 1359.
- (24) Lakowicz, J. R. *Principles of Fluorescence Spectroscopy*; Springer Science: Singapore, 2006.
- (25) Claborn, K.; Puklin-Faucher, E.; Kurimoto, M.; Kaminsky, W.; Kahr, B. *J. Am. Chem. Soc.* **2003**, *125*, 14825.

JP903598T

**The following resources related to this article are available online at [www.sciencemag.org](http://www.sciencemag.org) (this information is current as of November 16, 2009):**

**Updated information and services**, including high-resolution figures, can be found in the online version of this article at:

<http://www.sciencemag.org/cgi/content/full/314/5804/1437>

This article **cites 23 articles**, 2 of which can be accessed for free:

<http://www.sciencemag.org/cgi/content/full/314/5804/1437#otherarticles>

This article has been **cited by** 25 article(s) on the ISI Web of Science.

This article appears in the following **subject collections**:

Chemistry

<http://www.sciencemag.org/cgi/collection/chemistry>

Information about obtaining **reprints** of this article or about obtaining **permission to reproduce this article** in whole or in part can be found at:

<http://www.sciencemag.org/about/permissions.dtl>

# Probing the Chiroptical Response of a Single Molecule

Ruthanne Hassey, Ellen J. Swain, Nathan I. Hammer, Dhandapani Venkataraman, Michael D. Barnes\*

Chirally sensitive measurement techniques have generally been restricted to bulk samples. Here, we report the observation of fluorescence-detected circular dichroism (FDCCD) from single (bridged-triarylamine) helicene molecules by using an excitation wavelength (457 nanometers) in the vicinity of an electronic transition that shows circular dichroism in bulk samples. The distributions of dissymmetry ( $g$ ) parameters by analysis of signals from pure  $M$ - and  $P$ -type diastereomers are almost perfect mirror images of one another, each spanning a range of both positive and negative values. In addition, we observe a well-defined structure in the histogram of dissymmetry parameters suggestive of specific molecular orientations at the polymer interface. These single-molecule results highlight strong intrinsic circular dichroism responses that can be obscured by cancellation effects in ensemble measurements of a randomly oriented bulk sample.

Optical probes of chirality in organic systems are nearly as old as organic chemistry itself, tracing back to the early 1800s in initial studies of chiral natural products. Optical rotary dispersion and circular dichroism are now ubiquitous tools for characterizing and quantifying natural and synthetic chiral systems (1, 2). More sophisticated gas- and condensed-phase probes have recently brought fresh insights to the role of solvation and local dielectric environment in the problem of light-matter interactions with chiral materials (3–5). However, because conventional techniques for probing chiroptical properties of molecular systems are based on scattering or absorption, they necessarily require extensive ensemble averaging, thus obscuring information on the specific chiroptical signature for an individual molecule as well as the heterogeneity of the response associated with a particular system. Here, we report observation of fluorescence-detected circular dichroism (FDCCD) on individual helicene mol-

ecules deposited on the surface of a polymer film, and we show how the dichroism response is distributed for pure  $P$ - and  $M$ -type diastereomers. The measured distributions—each constructed from several hundred single-molecule measurements—are almost perfect mirror images of each other and are characterized by significantly larger average chiroptical response than observed in bulk solution. Surprisingly, the measured distributions span a range of dissymmetry parameters encompassing both positive and negative values. In addition, we find a well-defined structure in the histograms suggestive of specific molecular orientations at the polymer interface.

The chiroptical response of a molecular system is quantified by the dissymmetry parameter,  $g$ . In terms of fundamental molecular properties,  $g$  is defined as  $4R/D$ , where  $R = \text{Im}[(\langle \mathbf{g} | \boldsymbol{\mu} \rangle \langle \mathbf{e} | \mathbf{m} \rangle \langle \mathbf{g} |)]$ ,  $\langle \mathbf{e} |$  and  $\langle \mathbf{g} |$  are electronic states involved in the optical transition,  $\boldsymbol{\mu}$  and  $\mathbf{m}$  are the electric and magnetic dipole operators, and  $D = |\langle \mathbf{g} | \boldsymbol{\mu} | \mathbf{e} \rangle|^2$  is the dipole oscillator strength, thus giving the range of possible  $g$  values of  $\pm 2$  (6). Experimentally,  $g$  is determined by measured differential absorbance or luminescence intensity as  $g = 2[\epsilon_L - \epsilon_R]/[\epsilon_L + \epsilon_R]$ ; typically, ensemble-averaged values of  $g$  are quite small (0.01 to

0.001). Recently, significantly higher average dissymmetry values have been observed in aggregates of conjugated polymers with chiral side chains (7, 8), and experiments probing specific fine-structure components of  $^5D_0 \rightarrow ^7F_1$  transitions in Europium chelates have shown average  $g$  values between  $-0.7$  and  $-1.8$  (9). The latter result is particularly interesting in that such a large ensemble-averaged  $g$  value can be observed in such systems primarily because of the diminished sensitivity of inner-shell electronic transitions to environmental factors in rare earth ions. Thus, an important unresolved question is whether the generally weak chiroptical signature from molecular systems is a result of intrinsic molecular properties or the result of averaging over extrinsic heterogeneities such as molecular orientation or different local environments. Answers to these questions are vital to enhancing the purity of chiroptical response from a molecule of interest, thus potentially improving the practicability of such materials in device applications.

The power of single-molecule spectroscopy to disentangle heterogeneities in a complex physical system is well known (10–12). Many elegant published works on orientational dynamics (13), spectroscopy of conjugated polymers (14, 15), and quantum dot systems (16), for example, have shown how a molecule-by-molecule approach can provide detailed information on the photophysics of complex systems. Recently, Venkataraman, Riehl, and co-workers demonstrated the synthesis and bulk chiroptical characterization of a new kind of helicene molecule based on a bridged triarylamine structure (Fig. 1B) in which the right ( $P$ )– or left ( $M$ )–handed helical structure is enforced by the presence of a camphanate group at the indicated position (16). This camphanate group serves only to maintain chirality and does not absorb or emit light at the wavelengths used and therefore is not expected to contribute to the chiroptical properties of the helicene molecules. A very small ensemble-averaged circular polarized luminescence ( $\Delta\epsilon/\epsilon \approx 0.001$ ) was observed from solution-

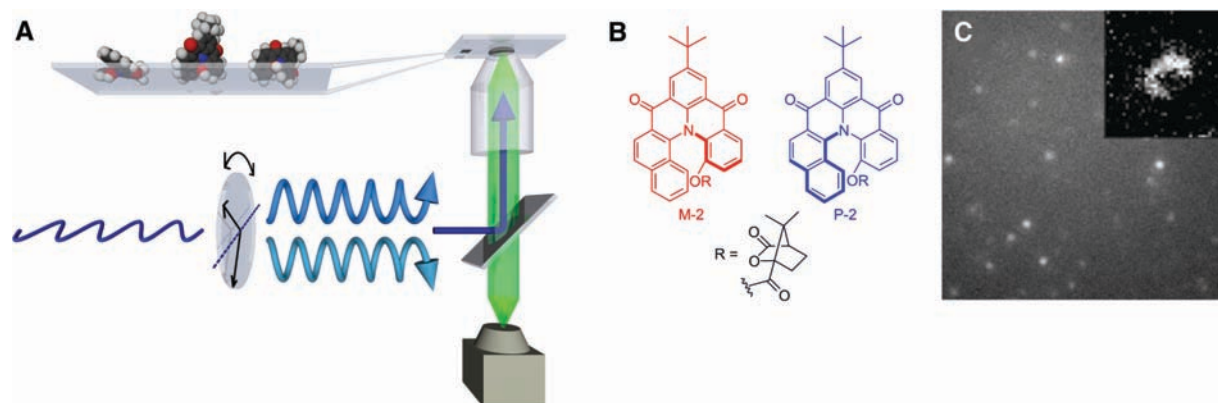


**Fig. 1.** (A) Experimental schematic. Linear-polarized laser radiation is periodically modulated between right- and left-handed circularly polarized light by rotation of a quarter waveplate. Fluorescence from single M2 or P2 molecules

(B) was collected in an epi-configuration with a 1.4-NA oil objective and high-sensitivity CCD camera. (C) Typical (in-focus) fluorescence image and defocused image (inset) from a M2 sample.

Department of Chemistry, University of Massachusetts-Amherst, Amherst, MA 01003, USA.

\*To whom correspondence should be addressed. E-mail: mdbarnes@chem.umass.edu

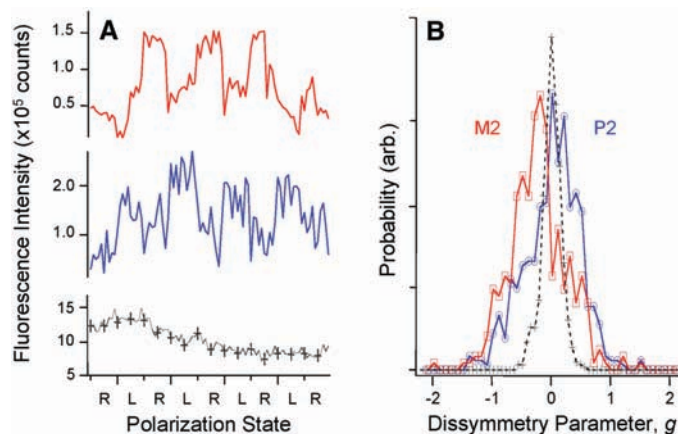
phase samples of these species (17), similar in magnitude to the circular dichroism at the same excitation wavelengths. Our approach here was to use ultradilute solutions to immobilize single helicene molecules at the surface of a polymer film and image the fluorescence-detected circular dichroism by using single-molecule spectroscopy and imaging techniques.

Figure 1A shows a schematic of our experimental apparatus, which is similar in many regards to that described by Kahr and co-workers for imaging circular dichroism in inorganic crystals (18). Using an epi-illumination configuration on a Nikon TE300 microscope with 1.4-numerical aperture (NA) objective, we delivered right- or left-handed circularly polarized light from a CW Ar<sup>+</sup> ion laser (457 nm; ~100 μW nominal power) to the sample by orienting a multi-order quarter waveplate (QWP) on a rotation stage at ±45° with respect to the (horizontal) input polarization axis, with 5 to 10 sequential charge-coupled device (CCD) camera exposures (Roper Scientific PhotonMax) for each QWP orientation (19). The molecules under study here were pure *M*- and *P*-type diastereomers of helicenes [as verified by <sup>1</sup>H-nuclear magnetic resonance (NMR)] derivatized with a camphanate moiety to enforce a specific chirality (Fig. 1B). Synthetic details are given elsewhere (20). For consistency in notation with respect to previously published work, we refer to the different diastereomers here simply as M2 and P2 (17). The 457-nm excitation wavelength excites transitions within the lowest electronic absorption band, where bulk solution and solid-film circular dichroism for these molecules are observed. Solutions of the two diastereomers were dissolved in semiconductor-grade methanol or cyclohexane and diluted to nominal concentrations of 10<sup>-11</sup> M; film-based samples were prepared by drop-casting ~200 μl of the ultradilute solution onto a thin polycycloolefin (Zeonex) polymer film. We find that the photochemical

stability of the helicenes is significantly enhanced by the use of a Zeonex supporting film over clean glass. In a typical fluorescence image obtained from such a sample, ~50 diffraction-limited fluorescent spots in a ~300-μm<sup>2</sup> area are seen, which show temporal instabilities (blinking and discrete photobleaching) characteristic of single molecules (Fig. 1C). The defocused image shown in the inset of Fig. 1C illustrates the bidirectional nature of the transition moment in these chiral species. Similar in nature to defocused images observed in quantum dot systems (21), the spatial fluorescence intensity patterns for the single helicene molecules are distinctly different from well-known defocused images of single linear dipoles or multichromophoric systems (22).

Figure 2A shows representative fluorescence intensity traces from the M2 and P2 helicenes under excitation with right- and left-handed circularly polarized laser radiation. In these examples, the sample is illuminated with alternating right- and left-circular polarized laser radiation every 10 frames, with a 1-s integration time per frame. The dissymmetry factor, *g*, in the single-molecule FDCD signal was defined as  $2[(I_L - I_R)/(I_L + I_R)]$ , where *I*<sub>R</sub> and *I*<sub>L</sub> are the measured fluorescence intensities associated with right or left circularly polarized excitation, respectively (23, 24). Single-molecule FDCD dissymmetry parameters were determined for each right and left circular polarization alternation cycle, and only fluorescent molecules with sufficient photochemical stability to follow intensity trajectories for at least 1.5 modulation cycles were used in the analysis. Although some variations in *g* are observed within a given single-molecule intensity trajectory, the gross value of *g* appears to be well defined for a given molecule during the measurement duration, suggesting that a particular single-molecule *g* factor is determined primarily by a predominantly static local environment.

**Fig. 2.** (A) Representative fluorescence intensity traces as a function of excitation polarization state for dye-doped polymer nanosphere (black), single P2 molecule (blue), and single M2 molecule (red). The dissymmetry parameters extracted from the P2 and M2 traces shown here were 0.54 and -0.63, respectively. (B) Normalized histograms of FDCD dissymmetry parameters determined from single-



molecule fluorescence measurements. The red curve with open squares represents data from M2, and the blue curve with open circles represents data from P2. For comparison, results from our control experiment with dye-doped 20-nm polymer nanospheres are shown (black curve with crosses). Data from ~500 single molecules were used in the construction of the histograms.

Plotted as histograms (Fig. 2B), the distributions of the dissymmetry parameter, *g*, obtained from single M2 and P2 molecules are notable mirror images of one another and appear to be the sum of a broad symmetric (about *g* = 0) component spanning a range of *g* ≈ ±1.3 and a much narrower component centered at *g* ≈ ±0.15. Even though the compounds were isolated as pure diastereomers, we considered the possibility that the unexpected shape of the distributions could be associated with the opposite diastereomer formed by partial isomerization in methanol solution, or by reaction with condensed water vapor on the film during sample preparation. However, further experiments starting from pure M2 powder under strict anhydrous conditions with cyclohexane showed that the broad distribution persisted. Thus, we conclude that the symmetric component present in both M2 and P2 *g* distributions at 457-nm excitation is a photochemical property of the molecular system and not the result of sample degradation. Our experimental bias toward molecules with higher photostability might, however, bias the distribution of dissymmetry parameters to higher (absolute) values.

The structure of the histograms is intriguing and suggests a nonrandom distribution of chiral axes at the polymer-air interface. Differences between normalized *g* distributions for P2 cast from methanol versus cyclohexane solutions are subtle and limited to the wings of the two

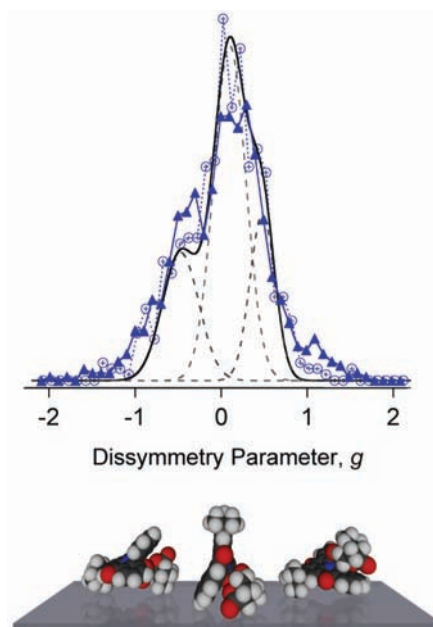


**Fig. 3.** Comparison of normalized dissymmetry parameter histograms for P2 dispersed from cyclohexane (dashed blue line and open circles) and methanol (solid blue line and triangles). The solid black curve is a fit to the P2/cyclohexane data with a three-component Gaussian fit. The lower graphic illustrates three different molecular orientations at the surface: camphanate-down, tripod, and camphanate-up.

distributions (Fig. 3) despite the solubility of Zeonex in the hydrocarbon but not the alcohol. Analysis of the M2 and P2 *g* distributions indicated three distinct components, with similar amplitudes but opposite signs for the two diastereomers. We propose that these three components are associated with three distinct stable molecular frame orientations at the surface shown in Fig. 3: camphanate down or up, and tripod (chiral axis perpendicular to the optical axis). These configurations correspond to the helicene frames parallel or perpendicular to the surface. We speculate that the opposite-handed component is associated with the “camphanate-up” orientation that places the helicene frame in direct contact with (or solvated by) the polymer film. Thus, the two in-plane orientations should be distinguishable from each other. Similar effects have been observed by Vaccaro and co-workers in cavity ringdown polarimetry measurements on (*S*)-(–)-propylene oxide, which show (for this particular system) that the specific rotation changes sign in the transition from the gas-phase to solvated molecule (3), illustrating the sensitivity of the chiroptical response to molecular environment. This effect is also analogous to the observation in crystals of tartaric acid of a variation in optical activity that is bisignate in nature (25). Here, we are restricted to molecular orientations induced by interactions with the substrate and as a result observe distinct contributions to the average *g* value. This result suggests that in solution phase, the measured *g* value represents a weighted average of all possible orientations and interactions with the solvent.

In summary, we observe that for a given bridged-triarylamine helicene diastereomer, there exists a significant probability of finding relatively large positive and negative *g* values whose distribution appears as a sum of three distinct components. We hope this result will spark further experimental and theoretical efforts in the study of individual chiral fluorophores. Our work demonstrates the feasibility of interrogating the fundamental nature of the interaction of light with chiral molecules at the single-quantum system level and provides valuable insights into the photophysics of chiral fluorophores. This result may also pave the way to the development of advanced new materials for efficient polarized light-emitting diodes (POLEDs) in next-generation display technologies (26).

#### References and Notes

- M. Srinivasarao, *Chem. Rev.* **99**, 1935 (1999).
- N. Berova, K. Nakanishi, R. W. Woody, Eds., *Circular Dichroism: Principles and Applications* (Wiley-VCH, New York, ed. 2, 2000).
- T. Muller, K. B. Wiberg, P. H. Vaccaro, *J. Phys. Chem. A* **104**, 5959 (2000).
- M. Y. Sfeir *et al.*, *Science* **312**, 554 (2006).
- R. Fasel, M. Parschau, K. H. Ernst, *Nature* **439**, 449 (2006).
- Contributions from electric dipole–electric quadrupole interactions that enter into the chiroptical response at the same order of perturbation theory as electric dipole–magnetic dipole interactions in the absence of ensemble averaging are expected to be small.
- A. Satrijo, S. C. J. Meskers, T. M. Swager, *J. Am. Chem. Soc.* **128**, 9030 (2006).
- J. N. Wilson *et al.*, *J. Am. Chem. Soc.* **124**, 6830 (2002).
- R. W. Schwartz, H. G. Brittain, J. P. Riehl, W. Yeakel, F. S. Richardson, *Mol. Phys.* **34**, 361 (1977).

- W. E. Moerner, *J. Phys. Chem. B* **106**, 910 (2002).
- C. Bai, C. Wang, X. S. Xie, P. G. Wolynes, *Proc. Natl. Acad. Sci. U.S.A.* **96**, 11075 (1999).
- S. Nie, R. N. Zare, *Annu. Rev. Biophys. Biomol. Struct.* **26**, 567 (1997).
- A. P. Bartko, K. W. Xu, R. M. Dickson, *Phys. Rev. Lett.* **89**, 026101 (2002).
- Z. H. Yu, P. F. Barbara, *J. Phys. Chem. B* **108**, 11321 (2004).
- N. Kumar *et al.*, *J. Phys. Chem. B* **107**, 6252 (2003).
- M. Nirmal *et al.*, *Nature* **383**, 802 (1996).
- J. E. Field, G. Muller, J. P. Riehl, D. Venkataraman, *J. Am. Chem. Soc.* **125**, 11808 (2003).
- K. Claborn, E. Puklin-Faucher, M. Kurimoto, W. Kaminsky, B. Kahr, *J. Am. Chem. Soc.* **125**, 14825 (2003).
- The degree of circular polarization at the sample was determined to be >96%. Tests for artifactual FDCD performed on single  $\text{Dil}_{18}$  molecules randomly oriented in the *x-y* sample plane showed a distribution of dissymmetry parameters similar to that of the polymer nanosphere results.
- J. E. Field, T. J. Hill, D. Venkataraman, *J. Org. Chem.* **68**, 6071 (2003).
- X. Brokmann, L. Coolen, M. Dahan, J. P. Hermier, *Phys. Rev. Lett.* **93**, 107403 (2004).
- A. P. Bartko, R. M. Dickson, *J. Phys. Chem. B* **103**, 11237 (1999).
- J. P. Riehl, F. S. Richardson, *Chem. Rev.* **86**, 1 (1986).
- F. S. Richardson, J. P. Riehl, *Chem. Rev.* **77**, 773 (1977).
- D. Mucha, K. Stadnicka, W. Kaminsky, A. M. Glazer, *J. Phys. Condens. Matter* **9**, 10829 (1997).
- S. H. Chen *et al.*, *Nature* **397**, 506 (1999).
- Support from the U.S. Department of Energy Office of Basic Energy Sciences (grant 05ER15695), NSF-sponsored MRSEC, NSF CHE 0134287, and the Intelligence Community Postdoctoral Research Fellowship Program is gratefully acknowledged. E.J.S. acknowledges support from the Bates Summer Research Fellowship.

23 August 2006; accepted 16 October 2006

Published online 2 November 2006;

10.1126/science.1134231

Include this information when citing this paper.

## Organic Globules in the Tagish Lake Meteorite: Remnants of the Protosolar Disk

Keiko Nakamura-Messenger,<sup>1,2\*</sup> Scott Messenger,<sup>1</sup> Lindsay P. Keller,<sup>1</sup> Simon J. Clemett,<sup>1,3</sup> Michael E. Zolensky<sup>1</sup>

Coordinated transmission electron microscopy and isotopic measurements of organic globules in the Tagish Lake meteorite shows that they have elevated ratios of nitrogen-15 to nitrogen-14 (1.2 to 2 times terrestrial) and of deuterium to hydrogen (2.5 to 9 times terrestrial). These isotopic anomalies are indicative of mass fractionation during chemical reactions at extremely low temperatures (10 to 20 kelvin), characteristic of cold molecular clouds and the outer protosolar disk. The globules probably originated as organic ice coatings on preexisting grains that were photochemically processed into refractory organic matter. The globules resemble cometary carbon, hydrogen, oxygen, and nitrogen (CHON) particles, suggesting that such grains were important constituents of the solar system starting materials.

Carbonaceous chondrite meteorites contain rare micrometer-sized mineral grains from evolved stars (stardust) (1). These meteorites also contain remnants of interstellar organic matter, marked by anomalous H and N isotopic compositions. This material has under-

gone complex histories of processing, dilution, and isotopic exchange with solar system materials, obscuring its original chemical and physical state. Rare microscopic inclusions with highly anomalous H and N isotopic compositions occur in meteorites and interplanetary dust

particles (IDPs), suggesting that some interstellar organic materials have survived intact (2–4). However, analytical limitations have left the nature of these materials poorly known.

Tagish Lake is a meteorite whose chemistry and mineralogy are intermediate between CI and CM2 carbonaceous chondrites (5). It was collected immediately after its fall was witnessed, minimizing terrestrial contamination (5). It has been linked to outer belt asteroids from its orbit, reflectance spectrum, hydrated mineralogy, and abundant carbonaceous matter, having 2.6 weight percent organic carbon (5–7). Tagish Lake organic matter often occurs as submicrometer, hollow globules (8). Similar objects were first observed in meteorite extracts in 1961 (9) and have recently been reported in several carbonaceous chondrites (10). However, owing to analytical

<sup>1</sup>Robert M. Walker Laboratory for Space Science, Astro-materials Research and Exploration Science Directorate, NASA Johnson Space Center, Houston, TX 77058, USA.

<sup>2</sup>ESC Group/Jacobs Sverdrup, NASA Johnson Space Center, Houston, TX 77058, USA. <sup>3</sup>ESC Group/ERC Inc., NASA Johnson Space Center, Houston, TX 77058, USA.

\*To whom correspondence should be addressed. E-mail: keiko.nakamura-1@nasa.gov